This full text paper was peer reviewed at the direction of IEEE Communications Society subject matter experts for publication in the WCNC 2008 proceedings.

Minimum Symbol Error Rate Turbo Multiuser Beamforming Aided QAM Receiver

Shuang Tan, Sheng Chen and Lajos Hanzo

School of Electronics and Computer Science
University of Southampton, Southampton, SO17 1BJ, U.K.
{st104r,sqc,lh}@ecs.soton.ac.uk

***Abstract*— This paper studies a novel iterative soft interference cancellation (SIC) aided beamforming receiver designed for high-throughput quadrature amplitude modulation systems communicating over additive white Gaussian noise channels. The proposed linear SIC aided minimum symbol error rate (MSER) multiuser detection scheme guarantees the direct and explicit minimisation of the symbol error rate at the output of the detector. Based on the extrinsic information transfer (EXIT) chart technique, we compare the EXIT characteristics of an iterative MSER multiuser detector (MUD) with those of the conventional minimum mean squared error (MMSE) detector. As expected, the proposed SIC-MSER MUD outperforms the SIC aided MMSE MUD.**

I. Introduction

Iterative detection was proposed by Berrou *et al.* [1] in the context of turbo codes. This work has later been extended to serially concatenated codes [2] and then found its way into iterative detector designs, such as iterative equalisers [3]–[5] and iterative multiuser detectors (MUDs) [6]. Most studies consider the minimum mean square error (MMSE) soft interference cancellation (SIC) aided iterative receiver [4]–[6]. However, the MMSE algorithm does not guarantee the direct and explicit minimisation of the system's error ratio. Hence in references [7], [8] the bit error ratio (BER), rather than the mean square error (MSE) was minimised at the MUD's output for binary phase shift keying and quadrature phase shift keying signals. Minimum BER detectors are challenging to derive for higher-order quadrature amplitude modulation (QAM), but nonetheless, Yeh and Barry have succeeded in directly minimising the detector's output symbol error rate (SER) [9]. Recently, a novel minimum SER (MSER) beamforming assisted receiver has been developed for high-throughput QAM schemes [10].

The concept of extrinsic information transfer (EXIT) charts was introduced in [11]. This semi-analytic technique uses the mutual information between the inputs and outputs of the concatenated receiver components in order to analyse their achievable performance. For example, EXIT charts were employed in turbo equalisation in [5], while in [12] they were used for examining the convergence properties of a turbo MUD.

The financial support of the EU under the auspices of the Optimix project as well as that of the EPSRC UK is gratefully acknowledged.

The novel contribution of this treatise is that iterative SIC aided MSER beamforming is proposed for QAM signals and its performance is studied with the aid of multi-user EXIT charts. Note that the shifting properties and the symmetrical distribution of the output signal's probability density function (PDF), which are used in the derivation of the original MSER beamforming solution [10], are no longer valid in our iterative system. Therefore, we derive a new *a priori* information assisted MSER MUD suitable for the employment in the proposed iterative SIC aided receiver. The structure of this contribution is as follows. In Section II, we outline the signal model used, followed by the portrayal of our iterative beamformer design. The focus of Section III is the novel MSER soft-input soft-output (SISO) interference canceller advocated. Section IV introduces the EXIT chart principles. Our simulation results and EXIT chart analysis are presented in Section V, followed by our conclusions in Section VI.

II. System Description

A. Signal Model

The system supports K number of QAM users and each user transmits on the same angular carrier frequency ω. The receiver is equipped with a linear antenna array consisting of L elements, which have a uniform element spacing of $\lambda/2$, where λ is the wavelength. Assume that the channel is non-dispersive in both the angular and time domains, and hence does not induce intersymbol interference. Then the symbol-rate-sampled received signal can be expressed as $r_l(n) = \sum_{k=1}^{K} h_k s_k(n) e^{j\omega t_l(\theta_k)} + n_l(n)$ for $1 \le l \le L$, where h_k is the non-dispersive complex-valued channel coefficient of user k, $s_k(n)$ is the nth symbol of the kth user, $n_l(n)$ is a complex-valued additive white Gaussian noise process with $E[|n_l(n)|^2] = 2\sigma_n^2$, and $t_l(\theta_k) = \frac{\pi}{\omega}(l-1)\sin(\theta_k)$ is the relative time delay at array element l for the source signal of user k, with θ_k being the direction of arrival for user k. The received signal vector $\mathbf{r}(n) = [r_1(n)\ r_2(n) \cdots r_L(n)]^T$ is given by $\mathbf{r}(n) = \mathbf{H}\mathbf{s}(n) + \mathbf{n}(n)$, where $\mathbf{n}(n) = [n_1(n)\ n_2(n) \cdots n_L(n)]^T$, the transmitted symbol vector is $\mathbf{s}(n) = [s_1(n)\ s_2(n) \cdots s_K(n)]^T$ and the system matrix is denoted by $\mathbf{H} = [\mathbf{h}_1\ \mathbf{h}_2 \cdots \mathbf{h}_K]$, which is associated with the steering vectors $\mathbf{h}_k = [h_k e^{j\omega t_1(\theta_k)}\ h_k e^{j\omega t_2(\theta_k)} \cdots h_k e^{j\omega t_L(\theta_k)}]^T$, $1 \le k \le K$.

1525-3511/08/$25.00 ©2008 IEEE

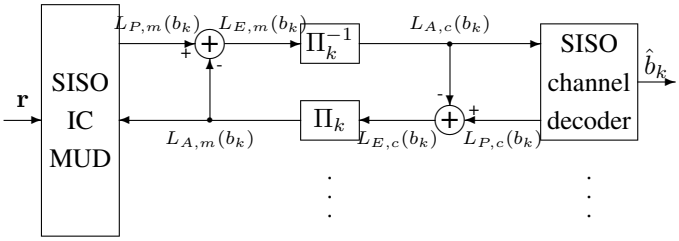

Fig. 1. Iterative multiuser beamforming receiver structure

B. Iterative Multiuser Beamforming Receiver Structure

The iterative multiuser beamforming receiver's structure is shown in Fig. 1, which consists of two stages, namely the SISO interference cancellation aided beamforming MUD, followed by K parallel single-user SISO channel decoders. The two stages are separated by the usual bit-based deinterleavers Π^{-1} and interleavers Π.

The proposed SISO beamforming MUD first determines the coefficients of the beamformer weight vector $\mathbf{w}_k(n)$ according to the specific design criterion employed and uses this weight vector for estimating the symbol $\hat{s}_k(n)$ corresponding to the transmitted symbol $s_k(n)$ from the received signal $\mathbf{r}(n)$ with the aid of a linear transformation. Let us now define $b_k(n,i)$ as the ith ($i \in \{1,\cdots,\log_2 M\}$) bit of the M-QAM symbol $s_k(n)$, whereas $b_k(j)$ is the same bit but in a different position of the bit-based interleaving block after the deinterleaver. $L_A(\cdot)$, $L_P(\cdot)$ and $L_E(\cdot)$ denote the *a priori*, *a posteriori* and extrinsic information in terms of logarithmic likelihood ratio (LLR), and the subscripts m and c are associated with the MUD and channel decoder, respectively. Then the SISO beamforming MUD delivers the *a posteriori* information of bit $b_k(n,i)$ expressed in terms of its LLR as [6]

$$\begin{aligned} L_{P,m}(b_k(n,i)) &= \ln \frac{\mathrm{P}[\hat{s}_k(n)|b_k(n,i)=0]}{\mathrm{P}[\hat{s}_k(n)|b_k(n,i)=1]} + \ln \frac{\mathrm{P}[b_k(n,i)=0]}{\mathrm{P}[b_k(n,i)=1]} \\ &= L_{E,m}(b_k(n,i)) + L_{A,m}(b_k(n,i)), \end{aligned} \quad (1)$$

where the second term, denoted by $L_{A,m}(b_k(n,i))$, represents the *a priori* LLR of the interleaved and encoded bits $b_k(n,i)$. The first term in (1), denoted by $L_{E,m}(b_k(n,i))$, represents the extrinsic information delivered by the SISO MUD, based on the received signal $\mathbf{r}(n)$ and the *a priori* information about the encoded bits of all users, except for the ith bit of the desired user k. The extrinsic information is then deinterleaved and fed into the kth user's channel decoder, which will provide the *a priori* information in the next iteration.

As seen in Fig. 1, between the banks of channel decoders and interleavers, we compute the extrinsic LLR based on the *a priori* information $L_{A,c}(b_k(j))$ provided by the SISO beamforming MUD for the SISO decoder as $L_{E,c}(b_k(j)) = L_{P,c}(b_k(j)) - L_{A,c}(b_k(j))$ [6], where the extrinsic information is gleaned from the surrounding encoded bits, excluding the specific bit considered [6]. After interleaving, the extrinsic information delivered by the channel decoders is fed back to the SISO MUD, as the *a priori* information concerning the encoded bits of all the users for exploitation during the next iteration.

III. SISO Interference Cancellation

Given the *a priori* LLRs, we first define the mean and variance based on the *a priori* information of the kth user's symbols for the QAM constellation as in [5]: $\bar{s}_k = \mathrm{E}[s_k]$ and $v_k = \mathrm{E}[|s_k|^2] - |\bar{s}_k|^2$, where the symbol-index n was dropped for notational convenience. When using the SIC principle, the estimated symbol of user k can be expressed as [5]

$$\hat{s}_k = \mathbf{w}_k^H(\mathbf{r} - \mathbf{H}\underline{\bar{\mathbf{s}}}_k), \quad (2)$$

where $\underline{\bar{\mathbf{s}}}_k = [\bar{s}_1 \cdots \bar{s}_{k-1}\ 0\ \bar{s}_{k+1} \cdots \bar{s}_K]^T$. In the next two subsections we outline the differences between the MSER MUD and the MMSE MUD.

A. SISO Interference Cancellation Using the MMSE MUD

Classically, the MMSE solution for the beamformer's weight vector $\mathbf{w}_k$ is expressed as [6]

$$\mathbf{w}_{k,mmse} = (\mathbf{H}\underline{\mathbf{V}}_k\mathbf{H}^H + E_s\mathbf{h}_k\mathbf{h}_k^H + 2\sigma_n^2\mathbf{I}_L)^{-1} \cdot E_s\mathbf{h}_k, \quad (3)$$

where E_s is the average symbol energy, $\mathbf{I}_L$ denotes the $L \times L$ identity matrix and $\underline{\mathbf{V}}_k = \mathrm{diag}[v_1 \cdots v_{k-1}\ 0\ v_{k+1} \cdots v_K]$, in which $\mathrm{diag}[\cdot]$ denotes a diagonal matrix.

As stated in [6], the conditional PDF $\mathrm{P}[\hat{s}_k|s_k{=}s^{(p)}]$, where $s^{(p)}$ is the pth ($p \in \{1,2,\cdots,M\}$) legitimate value of the QAM constellation, may be assumed to be Gaussian distributed and the corresponding extrinsic output LLR is given by [6]

$$L_E(b_k(i)) = \ln \frac{\sum_{\substack{\forall s^{(p)}:\\ b^{(p)}(i)=0}} \exp\left(\frac{-|\hat{s}_k - \mu_k^{(p)}|^2}{\sigma_k^2}\right) \prod_{\forall i' \neq i} \mathrm{P}(b_k^{(p)}(i'))}{\sum_{\substack{\forall s^{(p)}:\\ b^{(p)}(i)=1}} \exp\left(\frac{-|\hat{s}_k - \mu_k^{(p)}|^2}{\sigma_k^2}\right) \prod_{\forall i' \neq i} \mathrm{P}(b_k^{(p)}(i'))}, \quad (4)$$

where $b^{(p)}(i)$ denotes the ith bit of $s^{(p)}$, $\mu_k^{(p)} = s^{(p)}\mathbf{w}_k^H\mathbf{h}_k$, $\sigma_k^2 = E_s\mathbf{w}_k^H\mathbf{h}_k(1 - \mathbf{w}_k^H\mathbf{h}_k)$, and the *a priori* probability of the i'th bit in symbol s_k is $\mathrm{P}(b_k^{(p)}(i')) = \frac{1}{2}\big(1 + \mathrm{sgn}(\frac{1}{2} - b^{(p)}(i')) \cdot \tanh(\frac{L_A(b_k(i'))}{2})\big)$.

B. SISO Interference Cancellation Using the MSER MUD

In [10], the MSER algorithm is investigated when the MUD has access to no *a priori* information. Moreover, the weight vector $\mathbf{w}_k$ is rotated to make $\mathbf{w}_k^H\mathbf{h}_k$ real and positive. Under these conditions, the subset PDFs conditioned on the different values of the estimated signal $\hat{s}_k$, when all the M^K possible symbol combinations are transmitted, satisfy the shifting properties and are symmetrically distributed [10], which may be used to simplify the weight vector calculation. However, when the MUD is provided with *a priori* information, these properties are invalid and the MSER method of [10] cannot be applied directly to our iterative system. Hence in this subsection we introduce the *a priori* information aided MSER MUD to resolve this problem.

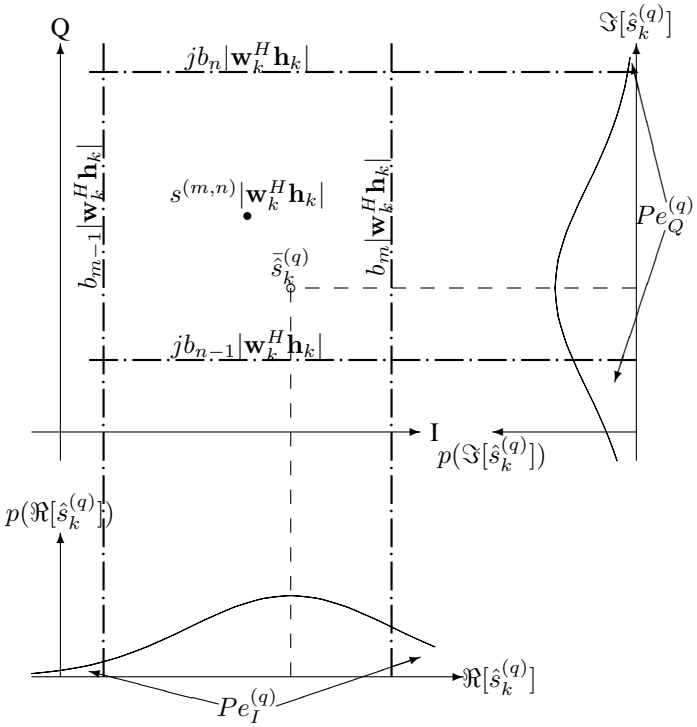

Fig. 2. Interference-affected expectation $\bar{\hat{s}}_k^{(q)}$ of the estimated signal $\hat{s}_k^{(q)}$ when $s_k^{(q)} = s^{(m,n)}$ and the decision boundaries

Let us define a symbol in the M-QAM constellation as $s^{(m,n)} = \gamma(2m - \sqrt{M} - 1) + j \cdot \gamma(2n - \sqrt{M} - 1)$, where $\gamma = \sqrt{3E_s/2(M-1)}$ and $1 \le m, n \le \sqrt{M}$. We assume that the qth ($q \in \{1, 2, \cdots, M^K\}$) symbol combination $\mathbf{s}^{(q)}$ is transmitted, in which the desired user k transmits symbol $s_k^{(q)} = s^{(m,n)}$. Fig. 2 shows the estimated signal $\hat{s}_k^{(q)}$ and its marginal PDFs under this condition. The PDF of $\hat{s}_k^{(q)}$ is a Gaussian distribution with a mean value $\bar{\hat{s}}_k^{(q)} = \mathbf{w}_k^H(\mathbf{H}\mathbf{s}^{(q)} - \mathbf{H}\underline{\mathbf{s}}_k)$, as seen in Fig. 2. When the kth user transmits symbol $s^{(m,n)}$, the conditional PDF of $\hat{s}_k$ is a scaled mixture of all the Gaussian PDFs in the subset $\{p(\hat{s}_k^{(q)}|s_k^{(q)}=s^{(m,n)})\}$, defined by

$$p(\hat{s}_k|s_k=s^{(m,n)}) = M \sum_{\substack{\forall \mathbf{s}^{(q)}: \\ s_k^{(q)}=s^{(m,n)}}} \underline{P}_k(\mathbf{s}^{(q)}) \cdot p(\hat{s}_k^{(q)}|s_k^{(q)}=s^{(m,n)})$$

$$= \frac{M}{2\pi\sigma_n^2 \mathbf{w}_k^H\mathbf{w}_k} \sum_{\substack{\forall \mathbf{s}^{(q)}: \\ s_k^{(q)}=s^{(m,n)}}} \underline{P}_k(\mathbf{s}^{(q)}) \cdot \exp\left(-\frac{|\hat{s}_k - \bar{\hat{s}}_k^{(q)}|^2}{2\sigma_n^2 \mathbf{w}_k^H\mathbf{w}_k}\right), \tag{5}$$

where $\underline{P}_k(\mathbf{s}^{(q)}) = \frac{1}{M}\prod_{\forall k' \neq k} \mathrm{P}(s_{k'}=s_{k'}^{(q)})$ is the probability of transmitting the qth possible QAM symbol combination $\mathbf{s}^{(q)}$, given the *a priori* information of the other $(K-1)$ users, except for user k. By defining $b_i = \gamma(2i - \sqrt{M})$ for $1 \le i \le \sqrt{M}-1$, the decision boundaries of $\hat{s}_k$ are determined by $b_i|\mathbf{w}_k^H\mathbf{h}_k|$ for the in-phase component and by $jb_i|\mathbf{w}_k^H\mathbf{h}_k|$ for the quadrature-phase component, as seen in Fig. 2. Then the error rate is the integral of the conditional PDF outside the corresponding boundaries. Fig. 2 only portrays the scenario of the inner constellation point, which is enclosed by boundaries. The points at the edge of the constellation may have open boundaries in one or two directions, which should be considered for the error rate calculation.

Let us now assume that the kth user transmits symbol $s^{(m,n)}$. Then the in-phase component's conditional error probability of $\Re[\hat{s}_k] \neq \Re[s^{(m,n)}]$ can be shown to be

$$Pe_I(s_k=s^{(m,n)})$$

$$= \begin{cases} \int_{b_1}^{+\infty} p(\hat{s}_k|s_k=s^{(m,n)})d\hat{s}_k, & m=1, \\ \int_{-\infty}^{b_{m-1}} p(\hat{s}_k|s_k=s^{(m,n)})d\hat{s}_k & \\ \quad + \int_{b_m}^{+\infty} p(\hat{s}_k|s_k=s^{(m,n)})d\hat{s}_k, & 2 \le m \le \sqrt{M}-1, \\ \int_{-\infty}^{b_{\sqrt{M}-1}} p(\hat{s}_k|s_k=s^{(m,n)})d\hat{s}_k, & m=\sqrt{M}, \end{cases}$$

$$= \begin{cases} M \sum_{\substack{\forall \mathbf{s}^{(q)}: \\ s_k^{(q)}=s^{(m,n)}}} \underline{P}_k(\mathbf{s}^{(q)}) \cdot \mathrm{Q}\left(\frac{b_1|\mathbf{w}_k^H\mathbf{h}_k| - \Re[\bar{\hat{s}}_k^{(q)}]}{\sigma_n\sqrt{\mathbf{w}_k^H\mathbf{w}_k}}\right), & \\ \qquad\qquad m=1, & \\ M \sum_{\substack{\forall \mathbf{s}^{(q)}: \\ s_k^{(q)}=s^{(m,n)}}} \underline{P}_k(\mathbf{s}^{(q)}) \cdot \left(\mathrm{Q}\left(\frac{\Re[\bar{\hat{s}}_k^{(q)}] - b_{m-1}|\mathbf{w}_k^H\mathbf{h}_k|}{\sigma_n\sqrt{\mathbf{w}_k^H\mathbf{w}_k}}\right)\right. & \\ \quad \left. + \mathrm{Q}\left(\frac{b_m|\mathbf{w}_k^H\mathbf{h}_k| - \Re[\bar{\hat{s}}_k^{(q)}]}{\sigma_n\sqrt{\mathbf{w}_k^H\mathbf{w}_k}}\right)\right), & 2 \le m \le \sqrt{M}-1, \\ M \sum_{\substack{\forall \mathbf{s}^{(q)}: \\ s_k^{(q)}=s^{(m,n)}}} \underline{P}_k(\mathbf{s}^{(q)}) \cdot \mathrm{Q}\left(\frac{\Re[\bar{\hat{s}}_k^{(q)}] - b_{\sqrt{M}-1}|\mathbf{w}_k^H\mathbf{h}_k|}{\sigma_n\sqrt{\mathbf{w}_k^H\mathbf{w}_k}}\right), & \\ \qquad\qquad m=\sqrt{M}. & \end{cases} \tag{6}$$

Similarly, the quadrature-phase component's conditional error probability of $\Im[\hat{s}_k] \neq \Im[s^{(m,n)}]$ can be shown to be

$$Pe_Q(s_k=s^{(m,n)})$$

$$= \begin{cases} M \sum_{\substack{\forall \mathbf{s}^{(q)}: \\ s_k^{(q)}=s^{(m,n)}}} \underline{P}_k(\mathbf{s}^{(q)}) \cdot \mathrm{Q}\left(\frac{b_1|\mathbf{w}_k^H\mathbf{h}_k| - \Im[\bar{\hat{s}}_k^{(q)}]}{\sigma_n\sqrt{\mathbf{w}_k^H\mathbf{w}_k}}\right), & \\ \qquad\qquad n=1, & \\ M \sum_{\substack{\forall \mathbf{s}^{(q)}: \\ s_k^{(q)}=s^{(m,n)}}} \underline{P}_k(\mathbf{s}^{(q)}) \cdot \left(\mathrm{Q}\left(\frac{\Im[\bar{\hat{s}}_k^{(q)}] - b_{n-1}|\mathbf{w}_k^H\mathbf{h}_k|}{\sigma_n\sqrt{\mathbf{w}_k^H\mathbf{w}_k}}\right)\right. & \\ \quad \left. + \mathrm{Q}\left(\frac{b_n|\mathbf{w}_k^H\mathbf{h}_k| - \Im[\bar{\hat{s}}_k^{(q)}]}{\sigma_n\sqrt{\mathbf{w}_k^H\mathbf{w}_k}}\right)\right), & 2 \le n \le \sqrt{M}-1, \\ M \sum_{\substack{\forall \mathbf{s}^{(q)}: \\ s_k^{(q)}=s^{(m,n)}}} \underline{P}_k(\mathbf{s}^{(q)}) \cdot \mathrm{Q}\left(\frac{\Im[\bar{\hat{s}}_k^{(q)}] - b_{\sqrt{M}-1}|\mathbf{w}_k^H\mathbf{h}_k|}{\sigma_n\sqrt{\mathbf{w}_k^H\mathbf{w}_k}}\right), & \\ \qquad\qquad n=\sqrt{M}. & \end{cases} \tag{7}$$

Then the average error probability of the in-phase and quadrature-phase components are given by

$$Pe_I = \frac{1}{M}\sum_{m=1}^{\sqrt{M}}\sum_{n=1}^{\sqrt{M}} Pe_I(s_k=s^{(m,n)}) \tag{8}$$

and

$$Pe_Q = \frac{1}{M}\sum_{m=1}^{\sqrt{M}}\sum_{n=1}^{\sqrt{M}} Pe_Q(s_k=s^{(m,n)}), \tag{9}$$

respectively. The resultant SER can be formulated as

$$Pe_s = Pe_I + Pe_Q - Pe_I \cdot Pe_Q. \tag{10}$$

Finally, the MSER solution is defined as the one that minimises the upper bound of the SER given by

$$\mathbf{w}_{k,mser} = \arg\min_{\mathbf{w}_k}(Pe_I + Pe_Q). \tag{11}$$

The upper bound $(Pe_I + Pe_Q)$ is very close to the true SER Pe_s because the term $Pe_I \cdot Pe_Q$ is typically negligible. In order to arrive at the optimum weights for the MSER solution, we need the gradients of Pe_I and Pe_Q in the context of the simplified conjugate gradient algorithm [7], which can be derived from the gradients of the Q-functions in Equations (6) and (7), leading to

$$\nabla_{\mathbf{w}_k} \mathrm{Q}\left(\frac{\Re[\bar{\hat{s}}_k^{(q)}] - b_i|\mathbf{w}_k^H\mathbf{h}_k|}{\sigma_n\sqrt{\mathbf{w}_k^H\mathbf{w}_k}}\right) = \frac{1}{\sqrt{2\pi}\sigma_n\sqrt{\mathbf{w}_k^H\mathbf{w}_k}} \cdot \exp\left(-\frac{(\Re[\bar{\hat{s}}_k^{(q)}] - b_i|\mathbf{w}_k^H\mathbf{h}_k|)^2}{2\sigma_n^2\mathbf{w}_k^H\mathbf{w}_k}\right) \cdot \left(\frac{\mathbf{w}_k(\Re[\bar{\hat{s}}_k^{(q)}] - b_i|\mathbf{w}_k^H\mathbf{h}_k|)}{\mathbf{w}_k^H\mathbf{w}_k} - \bar{\mathbf{r}}_k^{(q)} + \frac{b_i\mathbf{h}_k\mathbf{h}_k^H\mathbf{w}_k}{|\mathbf{w}_k^H\mathbf{h}_k|}\right) \tag{12}$$

and

$$\nabla_{\mathbf{w}_k} \mathrm{Q}\left(\frac{\Im[\bar{\hat{s}}_k^{(q)}] - b_i|\mathbf{w}_k^H\mathbf{h}_k|}{\sigma_n\sqrt{\mathbf{w}_k^H\mathbf{w}_k}}\right) = \frac{1}{\sqrt{2\pi}\sigma_n\sqrt{\mathbf{w}_k^H\mathbf{w}_k}} \cdot \exp\left(-\frac{(\Im[\bar{\hat{s}}_k^{(q)}] - b_i|\mathbf{w}_k^H\mathbf{h}_k|)^2}{2\sigma_n^2\mathbf{w}_k^H\mathbf{w}_k}\right) \cdot \left(\frac{\mathbf{w}_k(\Im[\bar{\hat{s}}_k^{(q)}] - b_i|\mathbf{w}_k^H\mathbf{h}_k|)}{\mathbf{w}_k^H\mathbf{w}_k} + j\bar{\mathbf{r}}_k^{(q)} + \frac{b_i\mathbf{h}_k\mathbf{h}_k^H\mathbf{w}_k}{|\mathbf{w}_k^H\mathbf{h}_k|}\right). \tag{13}$$

The marginal conditional PDFs $p(\Re[\hat{s}_k]|s_k{=}s^{(m,n)})$ and $p(\Im[\hat{s}_k]|s_k{=}s^{(m,n)})$ can both be assumed to be Gaussian distributed. Then the means and variances of the in-phase and quadrature-phase components of $\hat{s}_k$ are given by

$$\mu_{k,I}^{(m,n)} = \Re[s^{(m,n)}\mathbf{w}_k^H\mathbf{h}_k], \tag{14}$$

$$\mu_{k,Q}^{(m,n)} = \Im[s^{(m,n)}\mathbf{w}_k^H\mathbf{h}_k], \tag{15}$$

and

$$\sigma_{k,I}^2 = \Re[\mathbf{w}_k^H\mathbf{H}]\underline{\mathbf{V}}_{k,I}\Re[\mathbf{H}^H\mathbf{w}_k] - \Im[\mathbf{w}_k^H\mathbf{H}]\underline{\mathbf{V}}_{k,Q}\Im[\mathbf{H}^H\mathbf{w}_k] + \sigma_n^2\mathbf{w}_k^H\mathbf{w}_k, \tag{16}$$

$$\sigma_{k,Q}^2 = \Re[\mathbf{w}_k^H\mathbf{H}]\underline{\mathbf{V}}_{k,Q}\Re[\mathbf{H}^H\mathbf{w}_k] - \Im[\mathbf{w}_k^H\mathbf{H}]\underline{\mathbf{V}}_{k,I}\Im[\mathbf{H}^H\mathbf{w}_k] + \sigma_n^2\mathbf{w}_k^H\mathbf{w}_k, \tag{17}$$

where $\underline{\mathbf{V}}_{k,I} = \mathrm{diag}[v_{1,I}\cdots v_{k-1,I}\ \ 0\ \ v_{k+1,I}\cdots v_{K,I}]$, $\underline{\mathbf{V}}_{k,Q} = \mathrm{diag}[v_{1,Q}\cdots v_{k-1,Q}\ 0\ v_{k+1,Q}\cdots v_{K,Q}]$, with $v_{k',I} = \mathrm{E}[\Re^2[s_{k'}]] - \Re^2[\bar{s}_{k'}]$, $v_{k',Q} = \mathrm{E}[\Im^2[s_{k'}]] - \Im^2[\bar{s}_{k'}]$. By employing the assumption of Gaussian distribution, the computational complexity of the MSER MUD's output LLRs is simplified. The output extrinsic information delivered by the MSER MUD can be expressed as

$$L_E(b_k(i)) = \ln \frac{\sum_{\substack{\forall s^{(m,n)}:\\ b^{(m,n)}(i)=0}} \exp\left(\frac{-(\Re[\hat{s}_k]-\mu_{k,I}^{(m,n)})^2}{2\sigma_{k,I}^2}\right)\prod_{\forall i'\neq i}\mathrm{P}(b_k^{(m,n)}(i'))}{\sum_{\substack{\forall s^{(m,n)}:\\ b^{(m,n)}(i)=1}} \exp\left(\frac{-(\Re[\hat{s}_k]-\mu_{k,I}^{(m,n)})^2}{2\sigma_{k,I}^2}\right)\prod_{\forall i'\neq i}\mathrm{P}(b_k^{(m,n)}(i'))} \tag{18}$$

when $b_k(i)$ is mapped to the real part of s_k, and

$$L_E(b_k(i)) = \ln \frac{\sum_{\substack{\forall s^{(m,n)}:\\ b^{(m,n)}(i)=0}} \exp\left(\frac{-(\Im[\hat{s}_k]-\mu_{k,Q}^{(m,n)})^2}{2\sigma_{k,Q}^2}\right)\prod_{\forall i'\neq i}\mathrm{P}(b_k^{(m,n)}(i'))}{\sum_{\substack{\forall s^{(m,n)}:\\ b^{(m,n)}(i)=1}} \exp\left(\frac{-(\Im[\hat{s}_k]-\mu_{k,Q}^{(m,n)})^2}{2\sigma_{k,Q}^2}\right)\prod_{\forall i'\neq i}\mathrm{P}(b_k^{(m,n)}(i'))} \tag{19}$$

when $b_k(i)$ is mapped to the imaginary part of s_k, where $b^{(m,n)}(i)$ denotes the ith bit of $s^{(m,n)}$ and $\mathrm{P}(b_k^{(m,n)}(i')) = \frac{1}{2}\big(1 + \mathrm{sgn}(\frac{1}{2} - b^{(m,n)}(i')) \cdot \tanh(\frac{L_A(b_k(i'))}{2})\big)$.

IV. EXIT Chart Analysis

The EXIT chart analysis computes the mutual information (MI) between the LLRs and the corresponding bits, as detailed in [11]. An example of EXIT chart is shown in Fig. 3 for the simulated system investigated in Section V. Let I_A denote the MI between the *a priori* values L_A and the corresponding bit-sequence, while I_E denote the MI between the extrinsic values L_E and the corresponding bit-sequence. Then the EXIT function of the channel decoder is defined by $I_{E,c} = f_c(I_{A,c})$, which maps the input variable $I_{A,c}$ to the output variable $I_{E,c}$, and the specific value of $I_{E,c}$ in the range $[0, 1]$ characterises the quality of the output LLRs of the decoder components. Unlike in single-user turbo coding or turbo equalisation, in the multiuser detection scenario the MUD's EXIT curve recorded for the desired user depends on all the other $(K-1)$ users' channel decoder output MI. In our simulations all the users' SNRs are identical. Additionally, their angular locations are selected so that the relative time delay of all the users with respect to the angularly closest neighbors is the same. Hence the turbo MUD can average all the users' MIs in order to simplify the EXIT chart function to $I_{E,m} = f_m(I_{A,m}, E_b/N_0)$.

The output of one of the two constituent components is the input of the other, hence both transfer functions are shown in the same EXIT plane having coordinate axes of $(I_{A,m}{=}I_{E,c}), (I_{E,m}{=}I_{A,c})$. The stair-case-shaped lines in Fig. 3, connecting the MI points evaluated during each iteration, are referred to as the detection or decoding trajectory. The substantial advantage of EXIT charts accrues from the fact that the detection trajectory points recorded for both constituent components exchanging information fall on the continuous EXIT functions obtained independently in a separate process. An infinitesimally low BER may be attained, when there

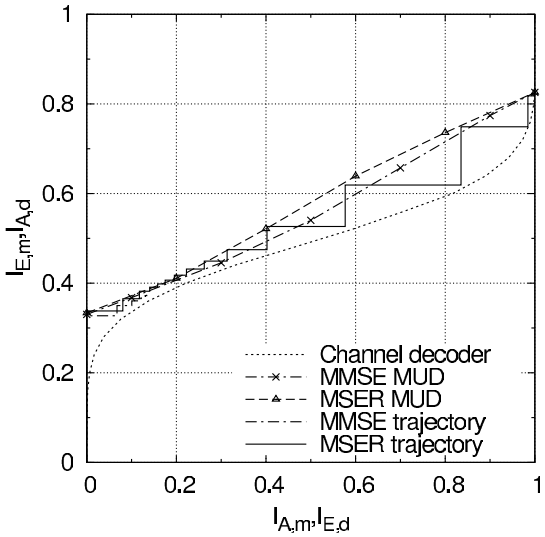

Fig. 3. EXIT charts and simulated trajectories of the iterative MMSE and MSER receivers supporting K=3 16QAM users at E_b/N_0=7.5 dB

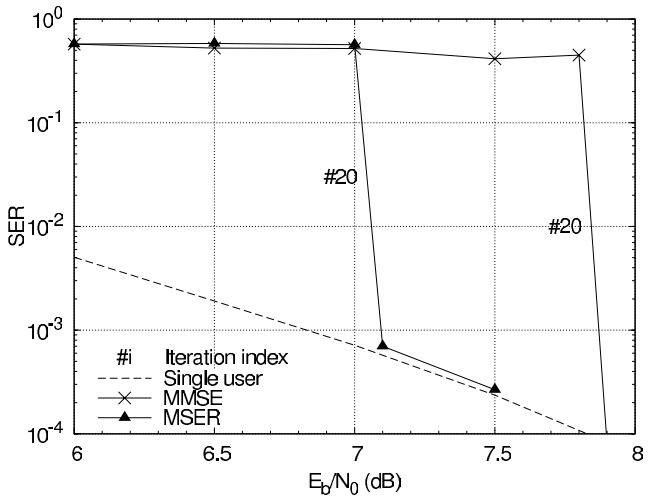

Fig. 4. SER comparison of the MMSE and MSER iterative beamforming receivers for the 16QAM system supporting K=3 users

is a so-called open tunnel between the EXIT curves of the decoder and the MUD. This graphical representation gives us an immediate insight into the number of detection iterations required for attaining the best possible BER performance.

V. Simulation Results

The system employs a two-element antenna array to support K=3 16QAM users. All the users have the same transmit power. Each user employs a different randomly generated interleaver. The interleaver length of each user is 2×10^4 bits. All the users have the same channel coefficients of $h_k = 1.0+j0.0$, $1 \leq k \leq 3$, and employ the same rate-$1/2$ and constraint-length 4 non-systematic convolutional code using the octally represented generators $(15, 17)$. The arrival angles of the users' signals are 68°, 15° and -24°, respectively.

Fig. 3 shows the EXIT curves and the simulated trajectories of the iterative MMSE and MSER 16QAM beamforming receivers supporting K=3 users at E_b/N_0=7.5 dB. In this 16QAM system, the MMSE and MSER MUDs have almost the same output $I_{E,m}$ value at both the axes at $I_{A,m}$=0 and $I_{A,m}$=1. Between these two points of intersection, the MMSE MUD has the lower EXIT curve, and the MSER's EXIT curve reaches a higher $I_{E,m}$ value.

Fig. 4 shows the SER versus SNR performance of the MMSE and MSER beamforming receivers, when supporting K=3 16QAM users in contrast to the single-user performance. It can be seen that after i=20 iterations, both the iterative systems approach the single-user performance. The MSER system has a lower operating SNR threshold, which is 0.8 dB lower than that of the MMSE system.

VI. Conclusion

This paper has introduced a novel SIC-MSER MUD employed in an iterative beamforming receiver designed for high-throughput QAM systems. This scheme directly minimises the SER instead of the MSE at the MUD's output, which leads to a better performance than that of the conventional MMSE-based systems at a cost of higher complexity. EXIT charts have also been used for analysing the convergence behaviour of the proposed system.

References

[1] C. Berrou, A. Glavieux and P. Thitimajshima, "Near Shannon limit error correcting coding and decoding: Turbo codes," in *Proceeding of IEEE International Conference on Communications* (Geneva, Switzerland), May 1993, Vol.2, pp.1064-1070

[2] S. Benedetto, D. Divsalar, G. Montorsi and F. Pollara, "Serial concatenation of interleaved codes: Performance analysis, design, and iterative decoding," *IEEE Transactions on Information Theory*, Vol.44, No.3, pp.909-926, May 1998

[3] C. Douillard, A. Picart, M. Jézéquel, P. Didier, C. Berrou and A. Glavieux, "Iterative correction of intersymbol interference: Turbo-equalization," *European Transactions on Communications*, Vol.6, pp.507-511, September-October 1995

[4] M. Tüchler, A. C. Singer and R. Koetter, "Minimum mean squared error equalization using *a priori* information," *IEEE Transactions on Signal Processing*, Vol.50, No.3, pp.673-6820, March 2002

[5] M. Tüchler, R. Koetter and A. C. Singer, "Turbo equalization: Principles and new results," *IEEE Transactions on Communications*, Vol.50, No.5, pp.754-767, May 2002

[6] X. Wang and H. V. Poor, "Iterative (Turbo) soft interference cancellation and decoding for coded CDMA," *IEEE Transactions on Communications*, Vol.47, No.7, pp.1046-1060, July 1999

[7] S. Chen, N. N. Ahmad and L. Hanzo, "Adaptive minimum bit error rate beamforming," *IEEE Transactions on Wireless Communications*, Vol.4, No.2, pp.341-348, March 2005

[8] S. Chen, L. Hanzo, N. N. Ahmad and A. Wolfgang, "Adaptive minimum bit error rate beamforming assisted receiver for QPSK wireless communication," *Digital Signal Processing*, Vol.15, No.6, pp.545-567, March 2005

[9] C.-C. Yeh and J. Barry, "Adaptive minimum symbol-error rate equalization for quadrature amplitude modulation," *IEEE Transactions on Signal Processing*, Vol.51, No.12, pp.3263-3269, 2003

[10] S. Chen, H.-Q. Du and L. Hanzo, "Adaptive minimum symbol error rate beamforming assisted receiver for quadrature amplitude modulation systems," in *Proceeding of IEEE Vehicular Technology Conference* (Melbourne, Australia), May 2006, Vol.5, pp.2236-2240

[11] S. ten Brink, "Convergence behavior of iteratively decoded parallel concatenated codes," *IEEE Transactions on Communications*, Vol.40, pp.1727-1737, October 2001

[12] K. Li and X. Wang, "EXIT chart analysis of turbo multiuser detection," *IEEE Transactions on Wireless Communications*, Vol.4, No.1, pp.300-311, January 2005